

# Images Collected from the Internet Reveal the Failing Mechanism of the Tailing Dam Breach at Kolontar, Hungary

**Jozsef Garai**, Retired Professor from the Department of Civil Engineering, University of Debrecen, Ótemető u. 2-4, 4028 Debrecen, Hungary; email: jozsefgarai29@gmail.com

**Imre Kovács**, College Professor at the Department of Civil Engineering, University of Debrecen, Ótemető u. 2-4, 4028 Debrecen, Hungary; email: <a href="mailto:dr.kovacs.imre@gmail.com">dr.kovacs.imre@gmail.com</a>

**ABSTRACT**: The failure of the red sludge tailing dam at Kolontar in 2010 was the most severe environmental disaster in the history of Hungary. The official investigations are confidential because the legal case has not been closed. The publicly accessible information from the breach of the dam are the photographs taken by the media and news agencies. Collecting these images and analyzing the recorded fractures and displacements of the dam reveal the failing mechanism. The breach of the dam resulted from failing to sliding, which had been developed in three stages. This conclusion is consistent with the observed movements of the dam deduced from a persistent scattered radar interferometry deformation analysis conducted between 2003 and 2010.

KEYWORDS: tailing dam breach, fracture pattern, case study, dam failing, red sludge disaster

SITE LOCATION: Geographic Database

### INTRODUCTION

The most severe environmental disaster in the history of Hungary occurred in 2010, when the red sludge tailing dam at Kolontar failed. The stored sludge was the byproduct of the aluminum production. According to the site operator (Magyar Alumínium Termelő és Kereskedelmi Zrt.), this sludge contained 40% to 45% Fe<sub>2</sub>O<sub>3</sub>, which was responsible for its red color; 10-15% Al<sub>2</sub>O<sub>3</sub>; 10-15% SiO<sub>2</sub>; 6-10% CaO; 4-5% TiO<sub>2</sub>; and 5-6% Na<sub>2</sub>O. Additionally, the liquid phase at pH 13 was found, representing 30% of the contents by mass. The Hungarian Academy of Sciences also identified traces of cadmium, chromium, mercury, nickel, lead, arsenic, and zinc.

The failure of the dam occurred on October 4th around noon. The dam broke over a 50 m length, resulting in the release of 1 million m<sup>3</sup> of highly basic sludge (Figures 1, 2). The flood of sludge killed 10 people and another 286 were injured (Banvolgyi, Gy., 2010).

Submitted: 11 March 2024; Published: 23 May 2025

Reference: Garai J., and Kovács I. (2025). *Images Collected from the Internet Reveal the Failing Mechanism of the Tailing Dam Breach at Kolontar, Hungary*. International Journal of Geoengineering Case Histories, Volume 8, Issue 1, 52 (2011) 10 4417/HGGH 20 21 24

p. 53-69, doi: 10.4417/IJGCH-08-01-04





Figure 1. The scale of the disaster: the highly toxic sludge flooded the neighboring villages in the valley of Torna. (Source: http://www.nydailynews.com/news/world/bodies-found-hungary-toxic-red-sludge-seeped-danube-river-article-1.188733.)

Following the disaster, many investigations have been conducted to find out what caused the failure of the tailing dam. The authorities classify the official investigations and the expert opinions. The investigators are bound by confidentiality agreements because the legal case has not been closed. The publicly available data, therefore, is very limited. However, the photographs taken by the media and news agencies following the breach of the dam are freely accessible from the Internet. Collecting these photos allowed the identification of all of the fractures of the dam. An analysis of these fracture patterns has been attempted to find out the failing mechanism leading to the breach of the dam.



Figure 2. Aerial photo of the breach of the tailing dam. (Source: https://www.ndtv.com/world-news/hungarys-toxic-sludge-spill-as-big-as-gulf-oil-leak-435094.)



### BUILDING TECHNOLOGY AND THE MATERIAL OF THE DAM

The dam is a hydraulic fill dam, which was built from slug and ash (Asboth, 2013). This fill material was the waste product of a nearby power plant. According to the technological instructions, the top soil of about 1 meter depth was removed and pushed to the side of the dam (Mecsi, 2013a). On both sides of the dam, 1.0-1.8 m high supporting earth structures were built and this base was filled with slug-ash. This supporting higher structure is required because the stabilization of the slug-ash requires a few days. The dam is therefore horizontally layered and inhomogeneous because of the quality change of the filling material (coarser or finer, etc.). The strength and other physical parameters of the sludge-ash fill, therefore, vary both horizontally and vertically.

The dam was built in two stages. In the first stage, between 1993 and 1995, the dam was built to about a height of 14 m. In the second stage the dam was completed. The filling of the reservoir had begun in 1998 and continued until the end of 2009. Resulting from slag-ash building technology, the crown of the dam was not evenly leveled out. In order to reach the maximum designed and licensed capacity, a 0.3-1.4 m additional layer on the top of the North dam of the reservoir was added in July 2010. (Turi et al., 2013) The final heights of the dams were between 25-27 m, supporting the 24 m high sludge (Farkas et al., 2013). The cross sections of the dams are not uniform (see Figure 3). The failed North dam has a smaller cross section than the West dam because an additional reservoir was planned to be built at the North side. It was assumed that the failed dam does not need to support horizontal load because the pressure of the stored sludge from the two sides would cancel out each other. The planned joint reservoir was never implemented.

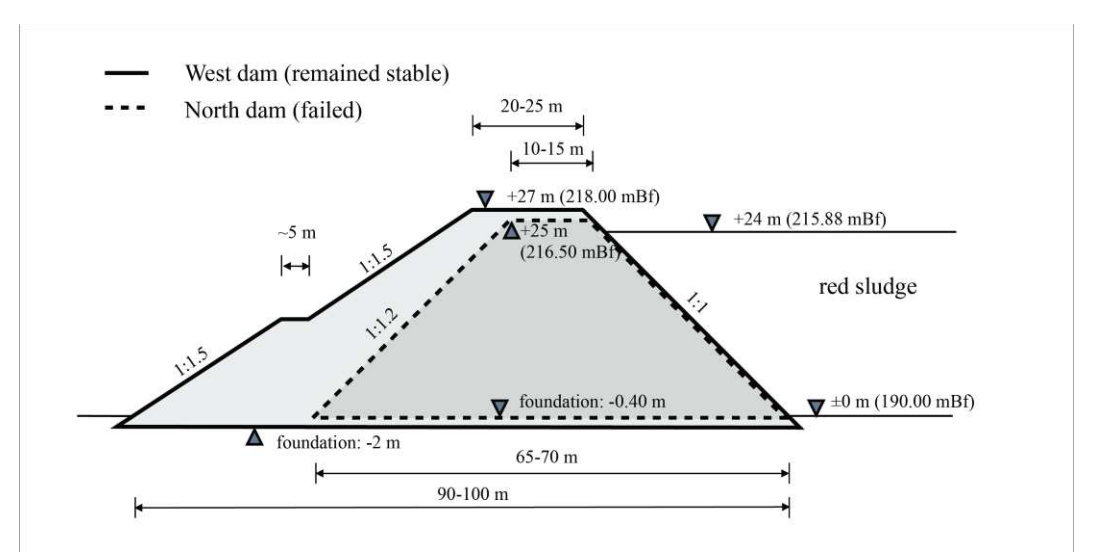


Figure 3. The cross sections of the North and West dams (Farkas et. al., 2013). The Northern dam primarily was designed to separate two reservoirs. The cross section of the dam therefore is significantly smaller in comparison to the West dam, which was designed to support the sludge pressure of the reservoir.

The designer of the dam tested the physical characteristics of hardened slug-ash before the construction (Mélyépterv, 1984). The internal friction ( $\phi$ ), cohesion (c), and tensile strength ( $\sigma_t$ ) used for the design of the dam were as follows:  $\phi = 40^\circ$ ; c = 50 KPa; and  $\sigma_t = 36$  KPa. Investigations made after the breach of the dam tested the unilateral compression ( $\sigma_c$ ) and tensile strength ( $\sigma_t$ ) of the fill. The average of the 29 tests were  $\sigma_c = 177$  KPa and  $\sigma_t = 67$  KPa, giving the parameters of the resistance  $\phi = 26^\circ$  and c = 54 KPa (Turai, 2013). The measured natural average density is 1.45 gcm<sup>-3</sup>.

The University of Miskolc also tested the strength of the fill and concluded that the unilateral compression strength test varied with grain size and depth (Mecsi, 2013b). The unilateral compression strength of the coarse grains and deeper samples were 0.5-0.8 MPa. These were reduced to 0.2-0.45 MPa closer to the surface. The unilateral compression strength of the fine grain samples were 1.5-2.5 MPa. The slag and ash has a relatively low unit weight of 15-15.5 KNm<sup>-3</sup>, and the dry unit weight is 7-8 KNm<sup>-3</sup>. The coarse grain material close to the surface of the dam has the smallest resistance, while the fine grain material deeper in the dam has the strongest resistance. The overall strength of the dam's material is relatively high due to the hydraulic chemical bond of the slug and the ash. Thus, the dam was built from a relatively rigid material which fails through fracturing.



### FRACTURES OF RIGID MATERIAL

The hydraulic chemical bond of the dam fill material makes the dam rigid and brittle. Rigid material fails along a well-defined surface resulting in detachment, known as fracture. Fracture is a fundamental mechanism of material failure. Two basic types of fractures can be identified in rock deformation experiments: extension (opening mode) fractures, and shears fractures (Jaeger & Cook, 1979; Paterson, 1978). The first one is caused by tensile stress, while the second one is the result of compression stresses. It has been shown that "hybrid fractures" between the extension and shear fractures occur from mixed stress states (Ramsey & Chester, 2004). The stresses and the related fracture patterns for extension, shear, and hybrid failures are shown in Figure 4.

### Coulomb-Mohr's theory of failure

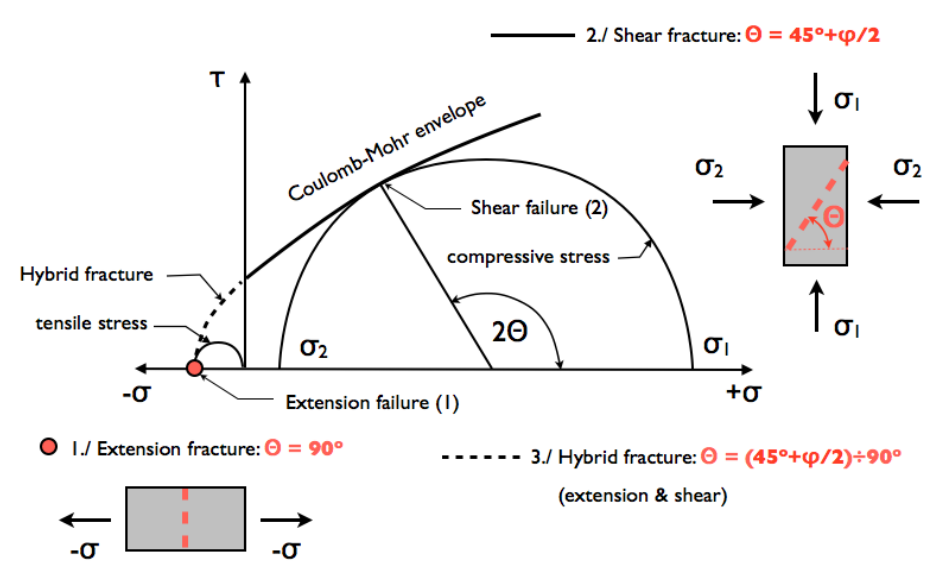
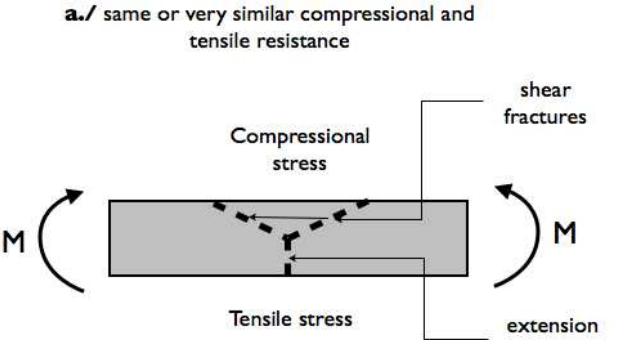


Figure 4. The two types of fractures are extension and shear. The dashed line shows the area where hybrid fractures occur, resulting from the transformation from extension to shear failure (Ramsey & Chester, 2004). The angles of the failed surface or fractures are given in relation to the principal stresses for the different failures.

In case of pure bending, compression and tensional stresses occur on the opposite sides of the beam. If the compression and tensile resistance of the substance is similar, then both extension and shear fractures are developing on the opposite sides of the beam (see Figure 5a).



### Characteristic fractures of pure bending



fracture

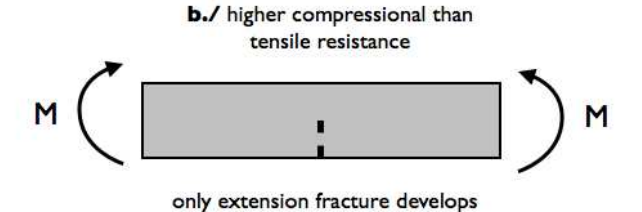


Figure 5. The fracture pattern of pure bending is shown. The tensile and compression stresses are on the opposite sides of the beam, developing extension and shear fracture respectively:

- (a) If the compression and tensile resistances of the substance are the same or similar to each other, then both shear and extension fractures are developing;
- (b) If the compression resistance of the substance is higher than the tensile resistance, then primarily extension fracture develops.

If the tensile strength of the substance is weaker than the compression, like rocks and concrete, then the tensile resistance of the substance is first exhausted and extension fracture develops (Figure 5b). If the bending is accompanied with shear stress, like a beam loaded in the middle, then a hybrid fracture pattern should develop (Melvin, 1993), as shown in Figure 6.

## Characteristic fractures of a beam subject to point load

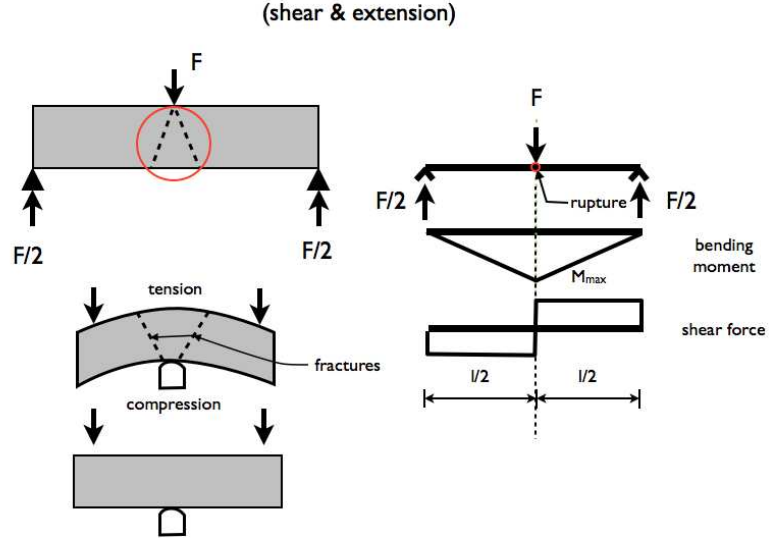


Figure 6. Combined extension and shear stress occurs in a beam when the load acts in the middle. This "bending force" produces hybrid fractures, resulting in a triangular or trapezoidal fracture shape (Melvin, 1993).



Identifying the fractures on a failed material allows one to identify the kind of stresses leading to the failure. The fractures can also be used to reconstruct the directions of the principle stresses. Knowing what kind of stress causes the failure and the directions of the principal stresses allows reconstructing the failing mechanism.

### DISPLACEMENTS OF THE FAILED DAM

Investigating the collected photos, five fracture locations had been identified. These locations are numbered I-V and shown in Figures 7 and 8. The entire dam section, between fracture Locations I and II, have been displaced. The section between Locations I and V is missing because it had been washed out by the outflow of the sludge. At Location I, the mark of the sludge on the surface of the exposed fracture shows that the displacement occurred at the breach (see Figure 7).

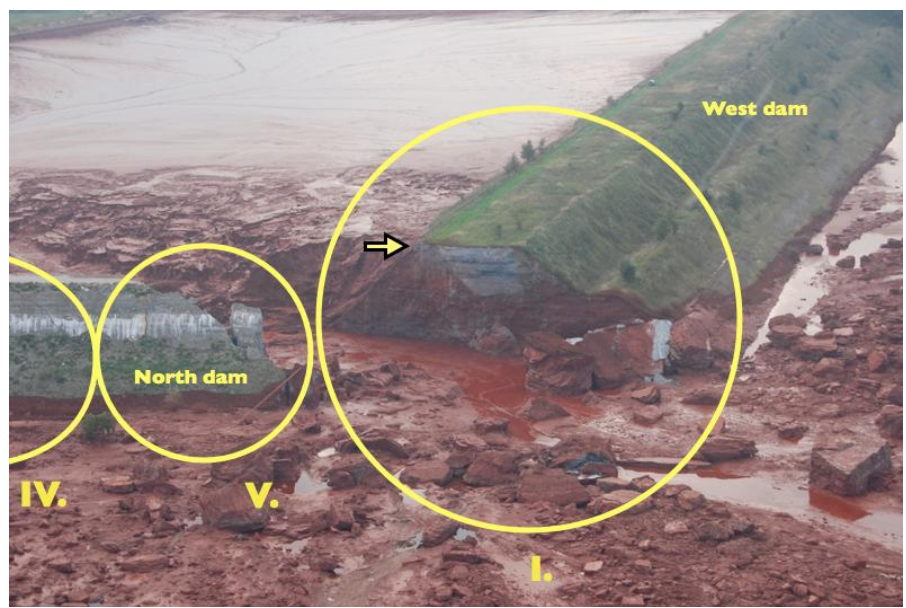


Figure 7. Photo showing the fracture Locations I, IV, and V. The red mark of the sludge on the open surface of the fracture at Location I is the same as the original sludge level. Thus, this fracture occurred right at the breach of the dam before the sludge level decreased in the reservoir.

(Source: https://www.aljazeera.com/photo\_galleries/europe/20101072047436735; http://www.kormany.hu/en/photo-galleries/negy-eve-tortent-a-vorosiszap-katasztrof.)

At Location V, the mark of the red sludge on the fracture (Figure 8) is lower than the original one, which indicates that this fracture occurred after the breach, when the sludge level in the reservoir was already lowered.



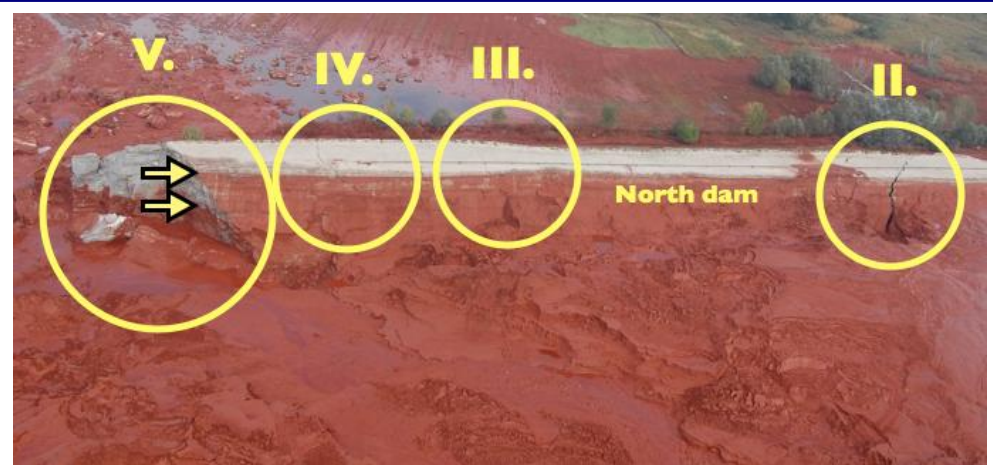


Figure 8. Photo showing fracture Locations II-V. The red mark of the sludge on the open surface of the fracture at Location V is shown. This mark is much lower than the original level in the reservoir, indicating that this fracture was formed after the breach, when the sludge level was significantly lower.

(Source: http://toleducation.org/achievements/red-legacy/.)

Displacements outward from the reservoir at Locations I and II of the western part of the North dam had been identified (Figure 9). The dam remained intact between these two locations; it is reasonable to assume that the entire dam section between them had been displaced. The displacements at the two ends of the failed dam section are different, which induced an angular distortion on the failed section. This distortion can be identified from the widening of the fracture at Location II (see Figure 9) and from the position of the detached pipe at Location II (see Figure 10). Thus, the failed section of the dam between Locations I and II has been displaced, and an angular distortion has been induced (Figure 9).

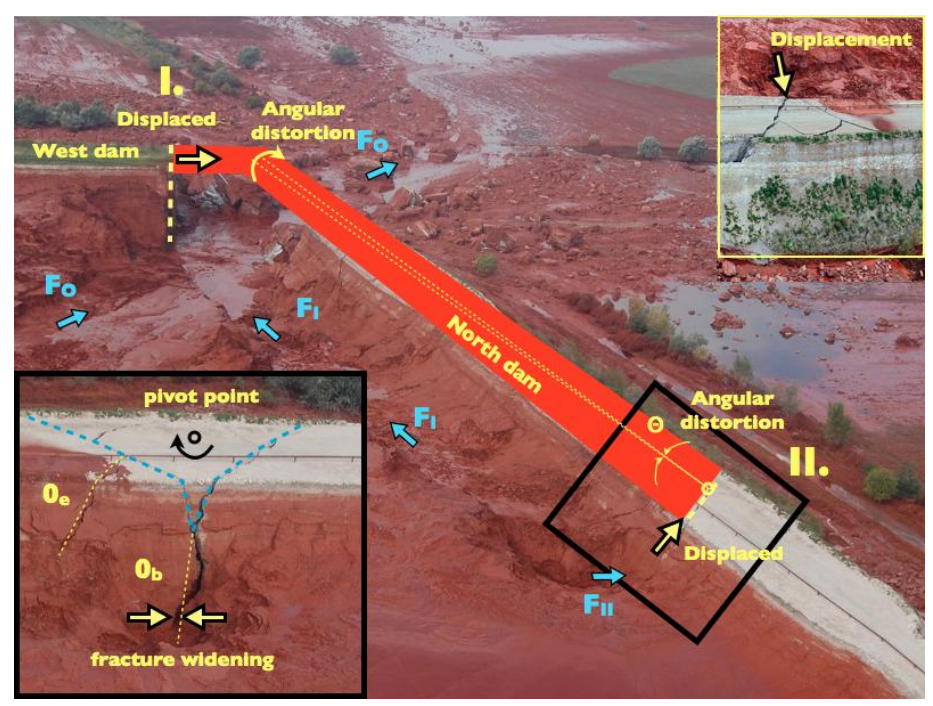


Figure 9. The failed section of the North dam is shown in red. This entire section had been displaced outward from the reservoir. Angular distortion also occurred from the bigger displacement at Location I. The widening of fracture  $0_b$  supports the angular distortion. The channels created by the outflow are visible on the surface of the red sludge. The identified flow directions (F) are shown.

(Sources: <a href="http://www.hungarianambiance.com/2011/09/possibility-of-act-of-terrorism-cant-be.html">http://www.hungarianambiance.com/2011/09/possibility-of-act-of-terrorism-cant-be.html</a> and <a href="https://phys.org/news/2011-04-wildlife-largely-absent-red-sludge.html#nRlv">https://phys.org/news/2011-04-wildlife-largely-absent-red-sludge.html#nRlv</a>.)



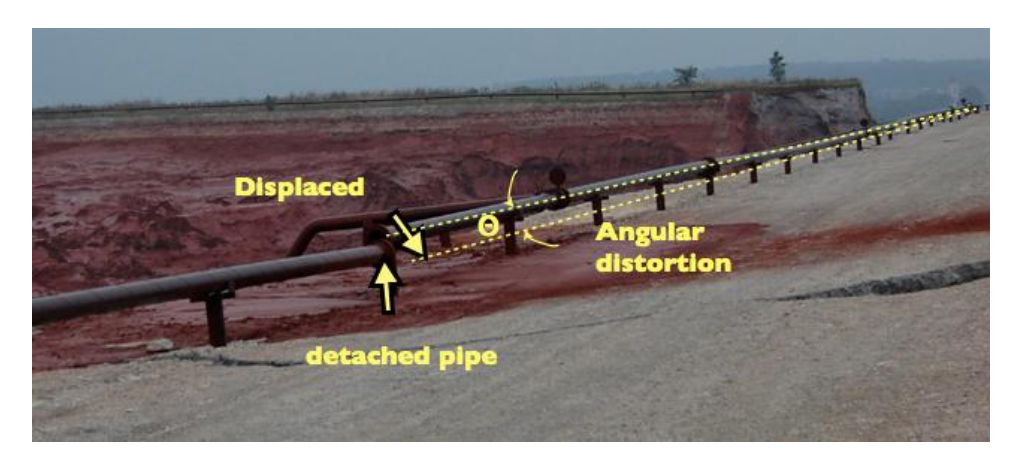


Figure 10. The angular distortion of the failed section of the dam can be seen from the position of the displaced broken pipe. On the failed part of the dam the pipe moved towards the reservoir despite the outward movement of the failed dam section. This indicates that the displacement resulting from angular distortion exceeded the outward displacement of the dam.

(Source: <a href="http://www.nbcnews.com/id/39610356/ns/world\_news-europe/t/human-negligence-toxic-sludge-boss-arrested/">http://www.nbcnews.com/id/39610356/ns/world\_news-europe/t/human-negligence-toxic-sludge-boss-arrested/</a>.)

### FLOW DIRECTIONS OF THE RED SLUDGE

The directions of the flow can be identified by a visual inspection of the surface of the red sludge in the reservoir on the photos. Three channels have been identified from the photos (Figure 11). These channels are also marked on Figure 9. It is obvious that the identified directions of the flaw points to the directions where the failed dam section has been detached and the openings occurred. It is assumed that a smaller opening created the narrower channel, while the wide channel relates to wider or bigger opening.



Figure 11. Based on the created flow channels in the red sludge, the flow directions were reconstructed. The initial flows  $F_1$  and  $F_2$  occurred at Locations I and II, pointing toward the direction of the existing fractures. The direction of flow  $F_1$  changed to  $F_0$  when the western part of the North dam had been washed away, creating a big opening. (Source: <a href="https://www.ndtv.com/world-news/hungarys-toxic-sludge-spill-as-big-as-gulf-oil-leak-435094">https://www.ndtv.com/world-news/hungarys-toxic-sludge-spill-as-big-as-gulf-oil-leak-435094</a>.)



The flow directions pointing towards Location I ( $F_I$ ) and Location II ( $F_{II}$ ) are narrow, indicating that these were the initial flows which were active right after the breach of the dam. These channels,  $F_I$  and  $F_{II}$ , are also deeper than the third one,  $F_O$ . The bigger depth of these channels indicates that these are the initial flows, when the initial hydraulic gradient was the highest. The flow directions further confirm that the fractures developed at Locations I and II initiated the breach of the dam. The third identified flow direction ( $F_O$ ) is shallower and wider, pointing toward the direction of the biggest opening. It is concluded that the flow  $F_I$  changed its direction to  $F_O$  when part of the North dam had been washed away.

### FRACTURES OF THE FAILED DAM

The five locations of the fractures can be seen in Figures 7 and 8. The individual fractures are numbered in the sequence of their occurrence. Minus and plus signs are used to indicate if the fractures occurred before or after the breach respectively. Number zero has been assigned to the fractures that occurred at the breach of the dam. The schematic patterns of the identified fractures and the assigned numbers are shown in Figure 12.

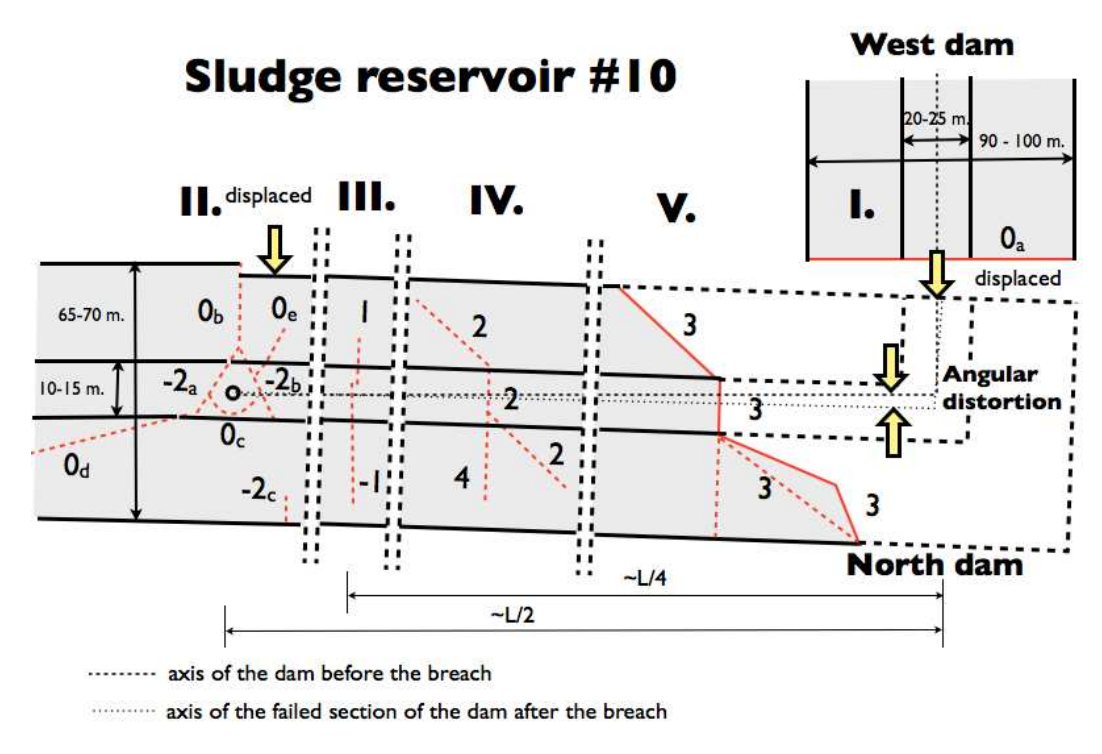


Figure 12. The sketch of the identified fractures is shown. The fractures are numbered in the sequence of their occurrence. Minus and plus signs are used to indicate if the fracture occurred before or after the breach respectively. Number zero has been assigned to the fractures that occurred at the breach of the dam.

### Location I

This location has one characteristic fracture  $(0_a)$ , which has been exposed at the breach (Figure 7). The fracture occurred at the corner of the North and West dams and its surface is perpendicular to the West dam. This fracture is clearly the result of tensional stress acting in the direction of the axis of the West dam. The fracture occurred at the breach because the marks of the red sludge on the exposed surface are at the same elevation as the original level in the reservoir (Figure 7). The North dam has been detached following the development of this fracture and displaced from the West dam, creating an opening. This opening was one of the initiators of the breach. The direction of the flow channel  $F_I$  is consistent with this conclusion.



### **Location II**

Location II is in the middle of the North dam. The fracture pattern is quite complex. Based on the fracture pattern, it can be identified that the fractures  $-2_a$  and  $-2_b$  relate to bending (Figure 6). The tension side of the bending was the outer side of the reservoir. However, on this side (outward from the reservoir), shear fractures  $0_c$  and  $0_d$  are also present, indicating compression stress on the same side (Figures 4 and 5).

# displaced location II. extension from bending hybrid from shear and tensile stress Angular distortion Oc hybrid from bending and shear stress shear fractures from angular distortion extension from bending and shear stress shear fractures from angular distortion extension from bending

Figure 13. The identified fractures at Location II are shown. Dashed circles mark fractures, formed from compression and tension in the same location. The coexistence of the extension and shear fractures in the same location can only be possible if the stress conditions changed in time.

The coexistence of compressional and tensional stresses at the same side of the dam is possible only if the stress conditions changed in time. At the breach, displacement and angular distortion occurred. These movements should develop compression stress on the outward and tensile stress in the inward side and shear stress. The bending related fractures  $-2_a$  and  $-2_b$  are not consistent with the stress condition at breaching, which indicates that these fractures  $-2_a$  and  $-2_b$  were already present when the breach occurred. The fracture pattern  $-2_a$  and  $-2_b$  is an indicative of failing from bending (Figure 6), which developed from the pressure of the red sludge acting from the reservoir site on the dam. The bending related fracture pattern is further supported by the location of the fractures, which is in the middle of the North dam, where the maximum bending moment should occur in a beam subject to uniform load (Figure 14).



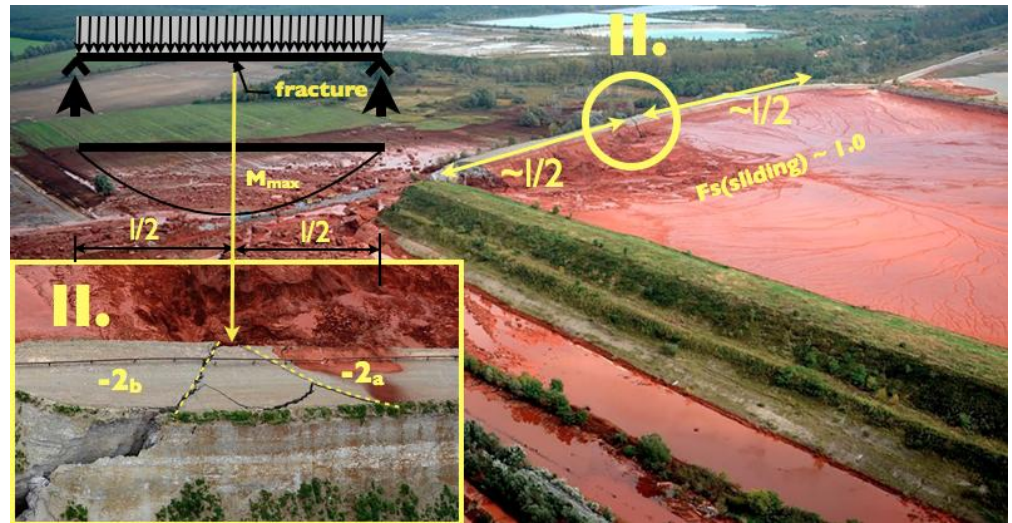


Figure 14. Location II is at the middle of the North dam, where the bending moment has its maximum under uniformly distributed load. The fracture pattern (Figure 6) and the location suggest that these fractures (-2<sub>a</sub>, and -2<sub>b</sub>) occurred from the bending. These fractures were formed before the breach of the dam.

(Sources: <a href="http://toleducation.org/achievements/red-legacy/">http://toleducation.org/achievements/red-legacy/</a>;

<a href="http://www.hungarianambiance.com/2011/09/possibility-of-act-of-terrorism-cant-be.html">http://www.hungarianambiance.com/2011/09/possibility-of-act-of-terrorism-cant-be.html</a>.)

The allowable angular distortion in buildings is 1/300 (Skempton and MacDonald, 1956). In masonry or concrete structures, fractures start to develop when the angular distortion exceeds this value, which might be too conservative for the dam because its material is not as rigid as these building materials. Using this conservative value on the approximately 500 m long dam, many decimeters of displacement in the middle of the dam were required to develop these fractures. Thus, the dam suffered a very significant deformation before the breach. The displacement occurred in the horizontal direction, indicating that, at the time of the fracture formation, the resistance against sliding was already exhausted. The developed fractures (-2a and -2b) reduced the bending moment at Location II close to zero, and the dam did not fail.

The last straw leading to the breach of the entire dam section was when the tensional resistance of the West dam was exhausted. The dam, whose sliding resistance had already been exhausted, had been detached at fracture  $0_a$  and the dam moved outward from the reservoir, activating the preexisting bending fractures at Location II. The displacement also induced an angular distortion which generated tensile and shear stresses on the reservoir side, resulting in fractures  $0_b$  and  $0_c$  respectively. The angular distortion of the dam produced compression stress at the outward site of the reservoir, which resulted in the development of shear fractures  $0_c$  and  $0_d$  on the outward side of the dam (Figure 15). The detachment occurred along the extension fracture  $0_b$  (Figure 9), and the preexisting fracture  $0_c$  (Figure 14). Fracture  $0_c$  (Figure 9) is a hybrid fracture caused by extension (angular distortion) and shear stresses (displacement).





Figure 15. Shear fractures ( $0_c$  and  $0_d$ ) caused by compressional stress at Location II are shown. These fractures were formed at the breach, resulting from the angular distortion of the failed dam section. On the opposite (reservoir) side, at the same time, extension fracture  $0_b$  occurred (Figure 9), extending the existing fracture of  $-2_b$ . (Sources: <a href="https://www.nbcnews.com/slideshow/toxic-red-sludge-floods-towns-near-budapest-39514793">http://www.nbcnews.com/slideshow/toxic-red-sludge-floods-towns-near-budapest-39514793</a>; <a href="https://www.hungarianambiance.com/2011/09/possibility-of-act-of-terrorism-cant-be.html">https://www.hungarianambiance.com/2011/09/possibility-of-act-of-terrorism-cant-be.html</a>).

### **Location III**

There are two independent fractures (1 and -1) perpendicular to the axis of the North dam. Based on the fracture direction, it is concluded that these fractures are the result of tensile stress acting in the direction of the axis of the dam (Figure 4). Both of these fractures resulted from bending, but there is a time gap between their occurrences. Following the development of fractures -2<sub>a,b</sub> at Location II, the maximum bending moment shifted from the middle of the dam to 1/4 of the length of the dam, which is where Location III is (Figure 16). The tensile strength relating to the bending moment of sludge pressure caused fracture -1 at the outward side of the dam. This failure occurred before the breach of the dam. At this weakened cross section, the angular distortion occurring at the breach and the additional flow pressures after the breach led to the development fracture 1 on the opposite side.



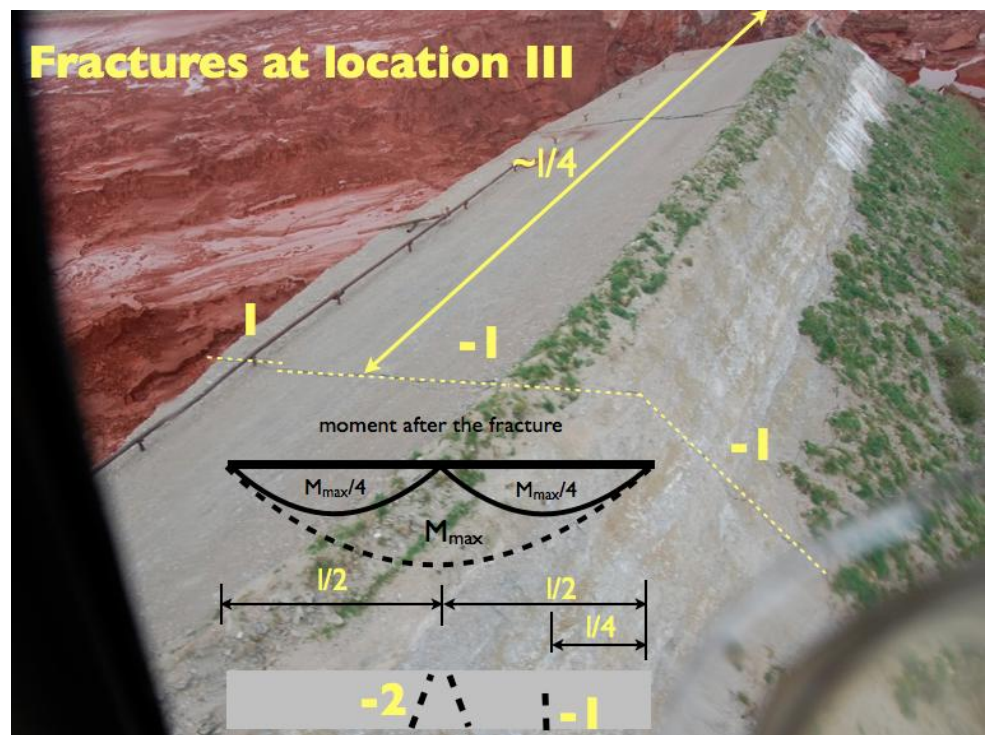


Figure 16. The location and the shape of fracture -1 is shown. Both the location and the shape of the rupture indicate that the failing was caused by bending. Following the formation of fractures -2 at Location II, the maximum moment was formed at Location III, resulting in the fracture of -1.

(Source: http://www.hungarianambiance.com/2011/09/possibility-of-act-of-terrorism-cant-be.html.)

### Locations IV and V

The fracture pattern of these sites shows hybrid failure (Figure 17).



Figure 17. The fractures at Locations IV and V are hybrid fractures caused by the outflowing pressure of the red sludge and the additional settlement. These fractures occurred after the breach of the dam and they have no relevance to the failing of the dam. (Source:

https://commons.wikimedia.org/wiki/File:Ajka accident d7df9fea08 b.jpg.)



If the fractures at Locations IV and V existed before the breach, then the transformation of the force and the torque would be very limited beyond these locations. Elimination of the torque would not allow the development of the angular distortion beyond Location IV or V. Thus, these fractures at Locations IV and V were formed after the breach. The mark of the red sludge on the surface of fracture 2 also shows that this failing occurred after the breach when the level of the red sludge was reduced from its original elevation (Figure 8). The widening of fracture 3 towards the top of the dam indicates that additional angular distortion in the vertical direction occurred, most likely resulting from the outflow of the sludge, which washed out the soil below the dam section at the opening. The settlement of the dam section led to the development of the extension fracture 4. All fractures at Locations IV and V had been developing after the breach of the dam; therefore, these fractures have no relevance to the breach. The list of all the fractures, as well as the type and the cause of the respective failure, is given in Table 1.

Table 1. The list of the fractures identified in the failed dam section. The proposed failing type and the

location #	fracture #	type of failure	cause of failure
I	$0_{\rm a}$	extension	tensile stress
II	-2 <sub>a,b</sub>	hybrid	bending and shear stress
II	$0_{b}$	extension	tensile stress from bending
II	$0_{ m c,d}$	shear	compression from angular distortion
II	$0_{\rm e}$	hybrid	shear and tensile stress
III	-1	extension	tensile stress from bending
III	1	extension	tensile stress from bending
IV	2	hybrid	compression from the sludge and tensile stress from settling
IV	4	extension	tensile stress
V	3	hybrid	compression from the sludge and tensile stress from settling

### **FAILURE ANALYSIS**

Based on the failure analysis of the collected photos, the failing mechanism of the tailing dam breach can be confidently reconstructed. The failure of the dam occurred in three stages. Stage 1 (#-2): the stored sludge pressure from the reservoir side at the location of the maximum bending moment caused fractures -2<sub>a,b</sub>. These fractures reduced the bending moment at Location II close to zero. Stage 2 (#-1): the developed new maximum bending moment at Location III resulted in fracture -1. The formation of these fractures required significant deformation of the dam. The development of fractures -2<sub>a,b</sub> t at the middle of the dam required many decimeter displacements. Thus, the factor of safety for sliding was already less than one at that time. Failing leading to a breach of the dam did not develop because the two ends of the "beam" were holding the sliding dam section in place. The combined resistance of the soil and the dam was not completely exhausted.

The catastrophic breach occurred at Stage 3 (#0), when the tensile resistance of the West part of the dam had also been exhausted and the entire dam between Locations I and II slid outward from the reservoir. The displacement was bigger at Location I, resulting in an angular distortion of the failed section. The created extension fracture at Location I and the fractures at Site II opened the reservoir, allowing the outflow of the stored red sludge. The flow enlarged the opening at Location I. The pressure of the flow broke and washed away the western part of the North dam between Locations I and V. The observed flow pattern on the surface of the sludge is consistent with this failing process. Fractures indicating vertical displacements before and at the breach have not been identified. Thus, bearing capacity failing of the dam did not occur.



The fracture patterns developed before and at the breach clearly identify horizontal displacements. Therefore, the failing mechanism of the dam was sliding. This conclusion is consistent with the persistent scattered radar interferometry deformation analysis, which measured 3.9 cm/year outward horizontal displacement of the North dam at the site of failure in the time period of 2003-2010.

### GEOTECHNICAL ASPECTS OF THE FAILURE

The soil profile under the dams at the site of Reservoir #10 is quite homogeneous. Under the dams, there is 0.5-4.0 m granular soil, and below that there is Pannonian fat clay (Mecsi, 2013b; Turai, 2013). The general soil profile is shown on Figure 18. Removing the topsoil, the dams were built on the top of the granular layer. This granular layer, with its high permeability, allowed the highly alkaline liquid to drain out into the groundwater. The groundwater monitoring wells detected this water pollution at the sites of the reservoirs VI-IX (built before reservoir #10) in the 1970s-1980s (Mecsi, 2013b). In order to stop further contamination into the groundwater, the reservoirs were sealed vertically with diaphragm and retaining walls. In different phases, starting in 1987, an overall 7,400 m retaining wall had been constructed (Turi et al., 2013). This project was completed in 2001.

The walls completely closed the entire reservoir area. Trenches inside and outside of the walls were built to collect the polluted water. Despite the sealing of the reservoirs, at Reservoir #10, which was still under operation, the highly alkaline water was leaching out. The pH value was 13 and higher (Turi et al., 2013). The strong alkaline condition significantly reduces the internal friction angle of the clay (Zeng et al., 2023). The long-term effect of the strong alkaline water, interacting with the Pannonian clay, has also changed the cations of the clay from calcium to sodium. This cation change further weakened the strength of the Pannonian fat clay at the interacting surface. The weak layer on the top of the clay had very low shear resistance. This was the reason why not only the failed section but also all of the dams of Reservoir #10 were slowly sliding outward from the reservoir.

The granular soil (sandy gravel) under the dams, with its weight and its bearing capacity at the toe of the dam, increased the resistance against sliding. Thus, the failure of the dam occurred where the thickness of the granular soil is the smallest (Ndagijimana, 2019). This conclusion is consistent with the failed section of the dam, where the granular layer was the thinnest (0,5 m) under the dam (Farkas et al., 2013). The dams with a bigger cross section had additional weights, which prevented the sliding failure, even though the resistance against sliding was nearly exhausted.

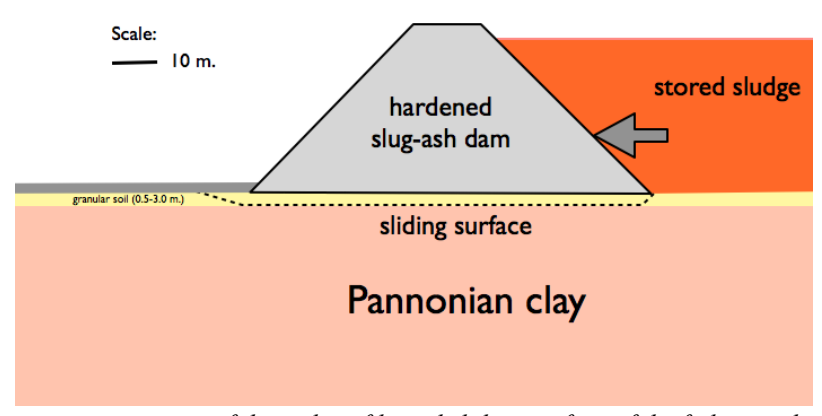


Figure 18. Schematic cross section of the soil profile and sliding surface of the failing is shown. The high pH and the cation exchange weakened the internal friction of the clay on the surface of the layer. The increasing horizontal pressure of the sludge on the dam led to the sliding failure of the dam along this weak resistant layer. The weight of the granular layer and its bearing capacity at the toe of the dam increased the resistance against sliding. Thus, failure of the dam occurred where the thickness of the granular layer was the thinnest.



### CONCLUSIONS

It can be concluded that the main contributing factor to the failure is the improper use of the dam. The North dam originally was designed to separate two reservoirs. Thus, it should not need to carry horizontal load or, if it does, it should be only a very limited one. The cross section of this dam, therefore, was significantly smaller in comparison to the West dam, which was designed to support the horizontal pressure of the sludge. The originally planned neighboring reservoir was not implemented, which changed the function of the North dam. The consequences of the modification of the construction schedule most likely had been overlooked. The North dam had not been redesigned or reinforced in order to carry horizontal load. Therefore, the dam failed due to sliding. The deformations of the dam preceding the breach were significant and could have been detected on-site with both land-based and space-based geodetic measurements several years before the breach occured. Careful site monitoring, such as visual inspection, could have also detected the fractures that occurred before the breach.

### **ACKNOWLEDGEMENTS**

The authors would like to thank the anonymous reviewers for their thoughtful comments and suggestions, which helped improve the quality of the manuscript.

### CONFLICT OF INTEREST

The presented research has not been supported by any funding or received any commissions. The authors, therefore, declare that they have no competing financial interests or personal relationships that could have appeared to influence the work reported in this paper.

### REFERENCES

- Asbóth, J. (2013). "Hidraulikus hányók geotechnikai és környezetvédelmi kérdései (Geotechnical and environmental questions of the hydraulic filled dams)." *Proc., 3rd Kézdi Konferencia*, 224-250. (in Hungarian)
- Banvolgyi, Gy. (2010). "Red mud storage dam failure in Hungary: the most serious accident of the Bayer process." Paper presented at 18th Int. Symp. ICSOBA, Zhengzhou, China.
- Farkas, J., Nagy, L., and Dudas, Zs. (2013). "A kolontári vörösiszap katasztrófa geotechnikai tanulságai." *Proc., 3rd Kézdi Konferencia*, 27-37. (in Hungarian)
- Grenerczy, G., and Wegmüller, U. (2011). "Persistent scatterer interferometry analysis of the embankment failure of a red mud reservoir using ENVISAT ASAR data." *Nat. Hazards*, 59, 1047. https://doi.org/10.1007/s11069-011-9816-6
- Grenerczy, G., and Wegmüller, U. (2013). "Deformation analysis of a burst red mud reservoir using combined descending and ascending pass ENVISAT ASAR data." *Nat. Hazards*, 65, 2205-2214. https://doi.org/10.1007/s11069-012-0470-4
- Jaeger, J. C., and Cook, N. G. W. (1979). Fundamentals of Rock Mechanics, Chapman and Hall, London, UK.
- Mecsi, J. (2013a). "Some technical aspects of a red mud reservoir embankment failure" In *Geotechnical Collapses, Understanding the Problems and Finding the Solution, ISSMGE, Hungarian National Committee, Kontraszt Plusz Kft., Pecs, Hungary*
- Mecsi, J. (2013b). "Technical Analyses and Lessons of the embankment failure at the Ajka red mud reservoir." *Proc.*, 7th Int. Conf. on Case Histories in Geotechnical Engineering, Chicago, USA, 3.47a, 1-11.
- Melvin, J. (1993). Accidental injury, Springer-Verlag, New York, USA.
- MÉLYÉPTERV. (1984). "Design guidelines for dams built by hydraulic technology (Irányelvek hidraulikus tározók tervezéséhez)." Budapest, Hungary. (in Hungarian)
- Ndagijimana, K. (2019). Application of Forensic Investigation in Assessing the Causes of the Red Sludge Disaster in Hungary. Thesis, University of Debrecen, Faculty of Engineering, Department of Mechanical Engineering, Debrecen, Hungary.
- Paterson, M. S. (1978). Experimental Rock Deformation—The Brittle Field, Springer, Berlin, Germany.
- Ramsey, J.M. and Chester, F.M. (2004). "Hybrid fracture and the transition from extension fracture to shear fracture." *Nature*, 428, 63-66.
- Skempton, A.W. and MacDonald, D.H. (1956). "The allowable settlements of buildings." *Proc., of the Institution of Civil Engineers*, London, UK, 5(3), 759–760.
- Turai, P. (2013). "FEM modelling of tailing dam (Zagytározó gátjának végeselemes modellezése)." OTDK 2013. (in Hungarian)



Turi, D., Pusztai, J., and Nyari, I. (2013). "Causes and Circumstances of Red Mud Reservoir Dam Failure In 2010 at MAL Zrt Factory Site in Ajka, Hungary." *Proc., Int. Conf. on Case Histories in Geotechnical Engineering*, 10. http://scholarsmine.mst.edu/icchge/7icchge/session03/10

Zeng, J., Ou, C., Zhang, J., Lu, K., Mo, K., Qin, S., Yang, B. (2023). "Influence of Different pH and Clay Content on the Mechanical Properties of Red Clay." *Open Access Library Journal*, 10, 1-8. doi: 10.4236/oalib.1110784

The open access Mission of the International Journal of Geoengineering Case Histories is made possible by the support of the following organizations:











The open access Mission of the International Journal of Geoengineering Case Histories is made possible by the support of the following organizations:









